Oxidation- and organic-molecule-induced changes of the Si surface optical anisotropy: *ab initio* predictions

2004 J. Phys.: Condens. Matter 16 S4323

(http://iopscience.iop.org/0953-8984/16/39/007)

INSTITUTE OF PHYSICS PUBLISHING JOURNAL OF PHYSICS: CONDENSED MATTER

J. Phys.: Condens. Matter **16** (2004) S4323–S4334 PII: S0953-8984(04)78673-7

Oxidation- and organic-molecule-induced changes of the Si surface optical anisotropy: *ab initio* predictions

W G Schmidt[1,4,5], F Fuchs[1], A Hermann[1], K Seino[1], F Bechstedt[1], R Paßmann[2], M Wahl[3], M Gensch[2], K Hinrichs[2], N Esser[2], S Wang[4], W Lu[4] and J Bernholc[4]

[1] Institut für Festkörpertheorie und -Optik, Friedrich-Schiller-Universität Jena, Max-Wien-Platz 1, 07743 Jena, Germany
[2] Institut für Spektrochemie und Angewandte Spektroskopie, Institutsteil Berlin, Albert-Einstein-Straße 9, 12489 Berlin, Germany
[3] Institut für Festkörperphysik, Technische Universität Berlin, Hardenbergstraße 36, 10623 Berlin, Germany
[4] Department of Physics, North Carolina State University, Raleigh, NC 27695-8202, USA

E-mail: wgs@ifto.physik.uni-jena.de

Received 31 March 2004, in final form 4 June 2004
Published 17 September 2004
Online at stacks.iop.org/JPhysCM/16/S4323
doi:10.1088/0953-8984/16/39/007

Abstract

In the last couple of years there has been much methodological and computational progress in the modelling of optical properties from *first principles*. Reflectance anisotropy spectra (RAS) can now be calculated with true predictive power and can thus be used to draw conclusions directly on the surface geometry. In the present work we study two potentially very interesting applications for RAS: the oxidation of Si(001) and the functionalization of the Si surface with organic molecules. Our calculations confirm experimental indications that the polarity of the interface-induced optical anisotropy is reversed layer by layer with increasing oxide thickness. The oscillation of the RAS amplitude should thus allow for the quantitative monitoring of the vertical progression of the oxidation. Our results for Si(001) surfaces modified by cyclopentene and 9,10-phenanthrenequinone adsorption show a strong sensitivity of the RAS signal with respect to the adsorption geometry. Comparison with experimental data shows that cyclopentene most probably adsorbs via a cycloaddition reaction with the Si surface dimers, while phenanthrenequinone seems to adsorb across two Si dimers.

1. Modelling of reflectance anisotropy

Optical spectroscopies are extremely valuable for *in situ*, non-destructive and real-time surface monitoring under challenging conditions as may be encountered, e.g., during epitaxial

[5] Author to whom any correspondence should be addressed.

growth. Reflectance anisotropy spectroscopy (RAS) is one of the plethora of surface sensitive spectroscopies probing linear optical coefficients which has been particularly successful in exploring surface structures. The high potential of RAS for growth monitoring was demonstrated by Kamiya *et al* [1] by measurements on GaAs(001) in ultra-high vacuum (UHV) as well as in atmospheric pressure of H_2, He and N_2. It was noted that each of the well known GaAs(001) surface reconstructions such as (4×4), (2×4) and (4×2) gives rise to a characteristic, fingerprint-like RAS spectrum. The correlation between reflection high-energy electron diffraction (RHEED) patterns and the RAS spectra allowed them to establish a database for GaAs(001) surface reconstructions [2]. The surface reconstruction can thus be determined *in situ*, even at ambient conditions. For many semiconductors a change of the surface reconstruction during layer growth occurs. RAS can therefore be easily used to monitor growth and layer completion. This application has proven highly successful [3, 4] and is now exploited commercially.

However, surface optical spectroscopies give only indirect information about the surface structure and chemistry. The intuitive interpretation of the spectra in terms of bond polarizabilities is difficult and often leads to wrong results even for relatively simple surfaces such as Si(001) (see discussion in [5]). Reliable calculations of surface optical spectra are needed to fully exploit their diagnostic potential. Following pioneering work by McIntyre and Aspnes [6] as well as Bagchi *et al* [7], Del Sole [8] obtained an expression for the surface contribution to the reflectance, $\Delta R/R$, where R is the reflectance according to the Fresnel equation. For s-light polarized along i and normal incidence he obtains

$$\frac{\Delta R_i}{R}(\omega) = \frac{4\omega}{c} \operatorname{Im}\left\{\frac{\Delta\epsilon_{ii}(\omega)}{\epsilon_{\mathrm{b}}(\omega) - 1}\right\}, \tag{1}$$

where ϵ_{b} is the bulk dielectric function, and

$$\Delta\epsilon_{ij} = \int \mathrm{d}z\,\mathrm{d}z'\,[\epsilon_{ij}(\omega; z, z') - \delta_{ij}\delta(z - z')\epsilon_0(\omega; z)] - \int \mathrm{d}z\,\mathrm{d}z'\,\mathrm{d}z''\,\mathrm{d}z'''\,\epsilon_{iz}(\omega; z, z')\epsilon_{zz}^{-1}(\omega; z', z'')\epsilon_{zj}(\omega; z'', z'''). \tag{2}$$

Here $\epsilon_{ij}(\omega; z, z')$ is the non-local *macroscopic* dielectric tensor of the solid–vacuum interface accounting for all many-body and local-field effects [9]. The second term in (2) is difficult to calculate because of the inversion required to obtain ϵ_{zz}^{-1} and because of the fourfold integration. It contains off-diagonal terms ϵ_{iz} of the susceptibility of the semi-infinite crystal. Manghi *et al* [10] investigated the influence of these terms for GaAs(110) and GaP(110) surfaces. No relevant contributions of the off-diagonal terms to the reflectance were noticed and they are therefore usually neglected. The first term of equation (2) can be evaluated by replacing the semi-infinite crystal by an artificial super-cell, large enough to represent the vacuum as well as the surface and bulk regions of the crystal under investigation. Provided that

(i) the slab is large enough to properly describe the surface region of the crystal, i.e., the surface as well as surface-modified bulk wavefunctions, and
(ii) the off-diagonal terms of the dielectric tensor are small compared to the diagonal ones,

a simple expression for the surface contribution to the reflectivity can be derived [10]

$$\frac{\Delta R_i}{R}(\omega) = \frac{4\omega}{c} \operatorname{Im}\left\{\frac{4\pi\alpha_{ii}^{\mathrm{hs}}(\omega)}{\epsilon_{\mathrm{b}}(\omega) - 1}\right\}. \tag{3}$$

Here $\alpha_{ii}^{\mathrm{hs}}(\omega)$ with $i = x, y$ is the diagonal tensor component of the averaged half-slab polarizability. It is important to note that under the conditions mentioned above, equation (3) contains in principle *all* surface contributions to the optical reflectance. This includes

contributions due to surface electronic states, atomic relaxations and the influence of the surface potential on the bulk wavefunctions as well as the surface local-field effects, i.e., the influence of the surface-modified microscopic fluctuations of the electric field on the macroscopic dielectric response, and many-particle effects such as the electronic self-energy and the electron–hole attraction. Of course, it is not an easy task to include all these contributions in practical calculations of the slab polarizability α.

Therefore, a comprehensive, quantitative picture of how surface optical anisotropies arise could only be obtained very recently, thanks to the advent of supercomputing and advanced numerical algorithms. Moreover, it is mainly limited to a few model cases such as clean and hydrogen covered Si surfaces [5, 11–15] or planes of III–V compound semiconductors [16–28]. Only very few theoretical works have been dedicated to clarifying the influence of the technologically relevant oxidation [29] and organic functionalization processes [30–32] on the RAS spectra of Si(001). In the present work we explore the potential of RAS for monitoring these processes by calculating the RAS spectra for the initial stages of the Si(001) surface oxidation as well as for energetically favourable configurations of 9,10-phenanthrenequinone (PQ) adsorbed on Si(001). Theoretical results for cyclopentene-adsorbed Si(001) surfaces obtained earlier by some of the present authors [30] are compared with measured data.

2. Computation

The calculations on oxidized and PQ-covered surfaces are performed using the Vienna *Ab initio* Simulation Package (VASP) implementation [33] of the gradient-corrected [34] density functional theory (DFT-GGA). The electron–ion interaction is described by the projector augmented-wave (PAW) method, allowing for the accurate quantum mechanical treatment of first-row elements with a relatively small basis set of plane waves. We expand the valence wavefunctions into plane waves up to an energy cut-off of 25 and 30 Ryd for PQ adsorbed and oxidized Si surfaces, respectively. We found these cut-off energies to be sufficient in extensive tests for organic molecules in the gas phase [35] and adsorbed on Si(001) [36] as well as for bulk SiO_2.

The Si(001) surface is modelled with a periodically repeated slab. The supercell consists of 12 atomic Si layers plus PQ molecules adsorbed on both sides (or including oxidized layers) and a vacuum region equivalent in thickness to eight atomic layers. The outermost five layers of the slab as well as the adsorbed molecules are allowed to relax. Brillouin zone integrations are performed using sets corresponding to 64 **k**-points in the full (1×1) surface Brillouin zone (SBZ).

The optical spectra are determined from all-electron wavefunctions obtained by the PAW method [37]. Transition matrix elements have been calculated for **k**-point sets corresponding to 256 points in the full SBZ. Earlier calculations have shown this **k**-point density to be sufficient to calculate a nearly converged RAS spectrum for the clean Si(001) surface [12]. The slab polarizability is calculated in the independent-particle approximation, i.e., neglecting excitonic and local-field effects. In the case of oxidized Si surfaces a scissors operator approach has been used to account for the bandgap underestimation of about 0.5 eV for bulk Si, which arises from the neglect of self-energy effects [38]. Calculations for smaller systems [13–15] have shown that many-body effects alter RAS spectra quantitatively rather than qualitatively, because RAS spectra are difference spectra, which are furthermore normalized to the bulk dielectric function (see equation (3)). Therefore, calculations within the independent-particle approximation reliably reproduce experimental data for a wide range of semiconductors [39]. The RAS spectra have been calculated from the slab polarizabilities according to equation (3). In order to compare with experiment, we consider the real part of the reflection amplitude r and use the approximation $\mathrm{Re}\,\frac{\Delta r}{r} = \frac{1}{2}\frac{\Delta R}{R}$.

The calculations for cyclopentene-covered Si(001) surfaces [30] were performed using a real-space multigrid implementation [40, 41] of DFT-GGA and non-local normconserving pseudopotentials [42].

3. Applications

3.1. Oxidized Si(001) surfaces

Atomically controlled oxidation of silicon surfaces is an eagerly desired technique in semiconductor device technology. It is indispensable to the realization of oxide layers with an atomic flatness and thickness. The oxidation reaction includes various elementary processes such as dissociation, adsorption, and diffusion of oxygen molecules through the surface, and bond formation between Si and O atoms near the surface or the interface. However, the microscopic phenomena and mechanisms of those processes are poorly understood. Of particular interest in that context is therefore the atom-scale monitoring of the oxidation, not only to clarify the growth mechanism, but also to control the layer thickness for microelectronic applications. Since light penetrates deeply into the Si substrate, i.e., of the order of 10^3 Å, RAS could in principle be used to monitor the formation even of deeply buried oxide layers, provided the oxidation gives rise to characteristic anisotropies. Based on tight-binding calculations that indicate that some of the oxidation-induced RAS signals change sign as the oxidation proceeds, Nakayama and Murayama [29] suggested that the layer thickness of oxidized Si can be measured with monolayer precision by monitoring and counting the spectral oscillations during layer-by-layer oxidation. Subsequently performed measurements by Yasuda *et al* [43, 44] showed that the polarity of the interface-induced optical anisotropy is indeed reversed repeatedly with increasing oxide thickness. In particular it was found that the negative anisotropy at the E_1 critical point energy of Si changes into a positive anisotropy upon oxidation of the first Si(001) monolayer. Oxidation of the second monolayer leads to a much weaker anisotropy at the E_1 critical point energy, with negative sign [43, 44]. Yasuda *et al* tried to explain their findings in the picture of dichroic threshold energies and broadening parameters for the bulk critical points [45]. However, not all experimentally found features could be explained (i.e. fitted) by introducing empirical anisotropies in the threshold energy and broadening parameter. Yasuda *et al* [43] furthermore point out that the oxidation-induced changes of the RAS signal cannot be accounted for by interface-related strain, which is often invoked to explain optical anisotropies at bulk critical point energies [46, 47]. The actual origin of the oxidation-induced RAS oscillations thus remained undetermined.

To model the initial stage of Si(001) surface oxidation we consider two energetically favoured surface structures, where oxidation occurs in the uppermost as well as in the uppermost and the second Si surface layer. The starting configurations for the atomic relaxation of these two structures are taken from a recent *first-principles* study on the energetics of Si(001) surface oxidation [48]. According to the notation of [48], these two models correspond to the $8a$ and $8/2a$ configurations. They are shown together with the clean Si surface in figure 1.

In order to verify the accuracy of our RAS calculations we first studied the optical response of the clean, c(4×2) reconstructed Si(001) surface. The calculated spectrum is shown with a solid curve in figure 2. A strong, dimer-state related minimum occurs at 1.7 eV. An additional minimum/maximum structure slightly below/above the E_1/E_2 critical point energy of bulk Si at 3.5/4.3 eV results from surface-modified bulk states. The calculated results are in excellent agreement with the data measured on highly oriented, single-domain Si(001) surfaces prepared by electro-migration [49]. Experimental spectra obtained for vicinal Si(001) surfaces [50, 51] show an additional feature at 3.0 eV that is due to surface steps [52, 12]. Also shown in figure 2 is the modification of the Si(001) RAS signal upon surface oxidation. It leads to the complete

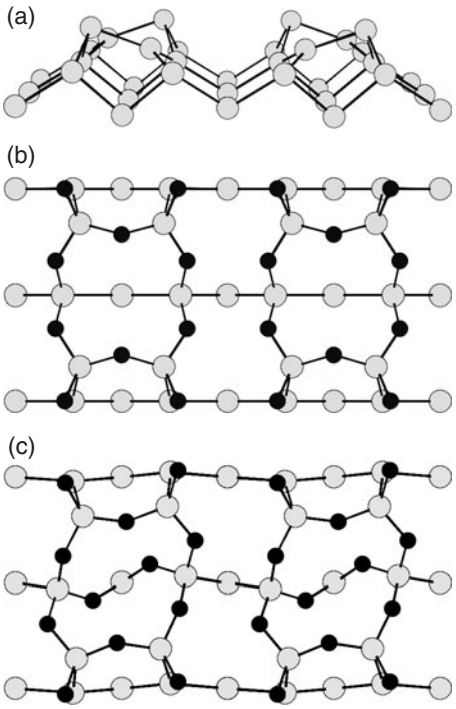

Figure 1. Perspective view of the clean relaxed Si(001) c(4 × 2) surface (a), and top view of the two models used to describe oxidation of the first (b) and of the first two Si(001) layers (c). Dark and grey symbols indicate O and Si atoms, respectively.

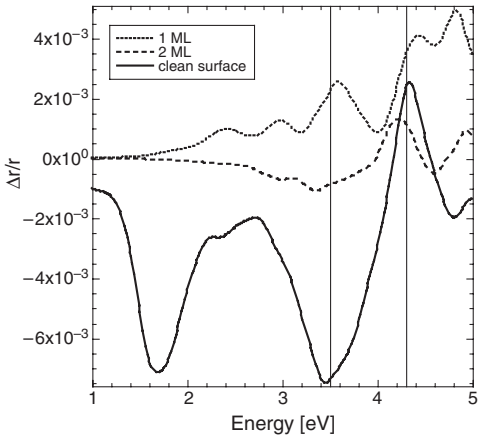

Figure 2. RAS spectra $[\mathrm{Re}\{(r_{[\bar{1}10]} - r_{[110]})/\langle r\rangle\}]$ calculated for the oxidized Si(001) configurations shown in figure 1 are compared with results for the clean surface. Thin lines are used to indicate the calculated positions of the E_1 and E_2 critical point energies.

cancellation of the 1.7 eV feature. This is to be expected, because both geometries used to describe the oxidation are characterized by O insertion into the Si surface dimers, and thus lead to the complete removal of Si-dimer-related surface states from the energy region of the fundamental gap. It is also in agreement with experiment, where the dimmer-related features are found to disappear upon exposing the Si(001) surface to O_2 at room temperature [43]. Oxidation of the first Si layer leads additionally to a reduction and a change in sign of the pronounced optical anisotropy at the E_1 critical point energy. This again is in very good agreement with experiment [44]. The description of the experiment is less convincing, though, for photon energies close to the E_2 critical point energy of Si: we find an enhancement of the E_2 peak, while a reduction of the anisotropy peak compared to the clean surface has been measured. The spectrum calculated for the oxidation of the second Si layer describes essential features of the experiment, namely the drastic reduction and sign reversal of the E_1 peak, but fails to model correctly the slightly negative anisotropy measured for photon energies close to E_2 [44]. However, when comparing experiment and theory it should be kept in mind that we model the oxidation of Si with only two well ordered surface structures, whereas the process actually involves a multitude of competing surface geometries and a high degree of surface disorder. It is likely that many more structural models need to be investigated in order to obtain a realistic picture of the oxidation process and its accompanying optical fingerprints. The fact that our simple approach reproduces the experimentally found layer-by-layer reversal of the anisotropy polarity at the Si E_1 energy is already very encouraging.

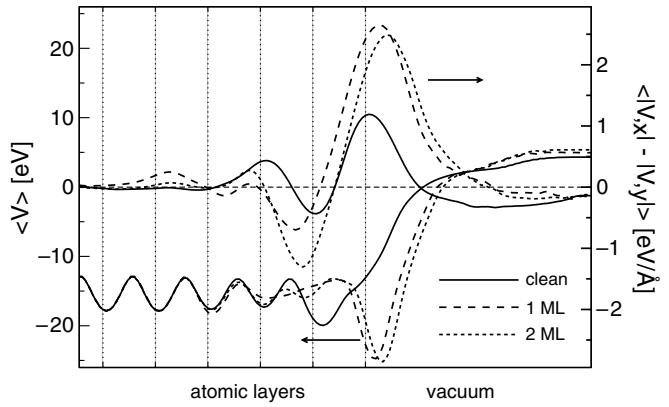

Figure 3. Averaged effective potential and its anisotropy for the clean and oxidized Si(001) c(4 × 2) surfaces shown along the surface normal. Dashed vertical lines indicate the positions of the atomic layers.

From experiment it was concluded that the oxidation-induced changes of the surface optical anisotropies are most likely unrelated to the strain at the SiO_2–Si interface [43]. This is confirmed by the present calculations, which were performed in supercells, the lateral dimensions of which were determined in Si bulk calculations, i.e., possible strain effects are excluded. Some of the present authors showed in an earlier computational study that the strain-related contribution to the RAS signal may actually be rather small [12]. Furthermore, we did not succeed in establishing a relation between characteristic RAS features and specific chemical bonds at the SiO_2–Si interface. Instead a large multitude of electronic states of predominantly bulk character was found to contribute to the optical anisotropies close to the E_1 and E_2 energies. This indicates that the oxidation-induced optical anisotropies arise predominantly in the Si bulk layers via an electronic coupling, at least in the energy range considered here. In order to illustrate this effect we consider the local part of the effective potential entering the DFT Kohn–Sham equations

$$V(\mathbf{r}) = V_{\mathrm{ps}}^{\mathrm{local}}(\mathbf{r}) + V_{\mathrm{H}}(\mathbf{r}) + V_{\mathrm{XC}}^{\mathrm{GGA}}(\mathbf{r}). \tag{4}$$

Here, $V_{\mathrm{ps}}^{\mathrm{local}}$ is the local part of the ionic pseudopotentials and V_{H} and $V_{\mathrm{XC}}^{\mathrm{GGA}}$ denote the Hartree and the exchange and correlation potential in the generalized gradient approximation (GGA), respectively. In order to quantify the change of this potential across the interface and surface region, we average the potential in the planes perpendicular to the surface normal. The resulting quantity

$$\langle V\rangle(z) = \frac{1}{A}\int_A \mathrm{d}x\,\mathrm{d}y\,V(x,y,z), \tag{5}$$

where A is the area of the surface unit cell, is shown in figure 3. The averaged potential $\langle V\rangle$ in the uppermost two to three atomic layers differs strongly from the value in the deeper layers. In order to quantify the anisotropy of the potential we consider the layer-averaged microscopic electric fields perpendicular to the surface normal. In detail, we calculate

$$\langle|\nabla_x V| - |\nabla_y V|\rangle(z) = \frac{1}{L}\int_{z-L/2}^{z+L/2}\mathrm{d}z'\,\frac{1}{A}\int_A \mathrm{d}x\,\mathrm{d}y\left\{\left|\frac{\partial V(x,y,z')}{\partial x}\right| - \left|\frac{\partial V(x,y,z')}{\partial y}\right|\right\}, \tag{6}$$

where L is the bilayer thickness and x/y are parallel to the $[110]/[\bar{1}10]$ direction. The difference (6) approaches zero only below the seventh atomic layer beneath the surface

(see figure 3). Obviously, the surface-induced anisotropy of the microscopic electric fields reaches far into the bulk. It therefore affects wavefunctions which cannot be categorized as electronic surface or interface states, but should rather be addressed as electric-field-modified Si bulk wavefunctions. The surface-induced deformations of these bulklike wavefunctions are weighted differently by the x and y components of the optical transition operator, leading to an anisotropic optical response from layers beneath the surface. Although these anisotropies might thus be considered as related to surface local fields, this is not true in a strict sense, because they already show up in the (0, 0) element of the microscopic dielectric tensor in reciprocal space. The local-field effects are not included in the present calculation, but have been shown earlier to be of minor importance, at least in the case of Si(001):H and Si(110):H surfaces [14, 13]. Comparing the layer-averaged microscopic electric field anisotropy of clean and oxidized Si surfaces in figure 3, one notices a layer- and coverage-dependent phase shift. While a direct proof appears very difficult, it seems at least plausible to attribute the RAS oscillations measured during the oxidation to these phase shifts.

3.2. Organic molecule adsorption on Si surfaces

Organic functionalization of semiconductors has become important for the development of new semiconductor-based devices. The physical and chemical properties of hybrid organic/inorganic materials depend crucially on the structural and chemical details of the interface. Techniques such as electron diffraction or scanning tunnelling microscopy (STM) give information on the order and symmetry of the organically modified surface [53]. However, they usually do not allow for discrimination between competing bonding scenarios. On the other hand, optical spectroscopies such as reflectance anisotropy spectroscopy (RAS) have been shown to be highly successful in the determination of semiconductor surface structures. At present, however, there are only very few studies that explore optical anisotropies of organically modified semiconductors experimentally [54–56] or computationally [30–32]. In particular, we are not aware of any study where measured and calculated optical anisotropies have been compared for organic molecule adsorption on a semiconductor surface.

The adsorption of cyclopentene (C_5H_8) on Si(001) was perhaps the first model case where the influence of organic molecules on the reflectance anisotropy of a semiconductor surface has been calculated [30]. The adsorption of cyclopentene on Si leads to what can be considered a prototypical alkene–Si(001) interface. It is experimentally well characterized by scanning tunnelling microscopy (STM) and by infrared and core-level spectroscopies [57, 58]. Some adsorption geometries have also been probed by cluster [59] and density-functional calculations [60, 61]. From experiment [57], two possible scenarios have been suggested for the reaction between Si(001) and a cyclopentene molecule: a [2 + 2] cycloaddition reaction, leaving the Si dimer intact, and an insertion reaction, where the Si dimer is broken (dimer-cleaved model). The reactions that leave the dimer intact result in 'dimerized' models and lead to a chemically saturated, but highly strained, interface geometry. This configuration can be classified further according to the positions of the hydrogen atoms in the direct vicinity of the Si surface. In the *trans*-type adsorption, the two H atoms are on alternating sides of the molecule, whereas both H atoms reside on the same side of the molecule in the *cis*-type configuration. On the other hand, a dimer cleavage reaction may occur which relieves the surface strain, but leaves unpaired electrons in the Si dangling bonds. The interface geometry is very sensitive to the presence of hydrogen: if atomic hydrogen is added near the Si surface atoms, both the dimerized and the dimer-cleaved configurations are found to relax toward a hydrogenated model [30]. The RAS spectra calculated in [30] for the hydrogenated model, the dimerized structure in *cis* and *trans* configurations and the dimmer-cleaved structure of the monolayer

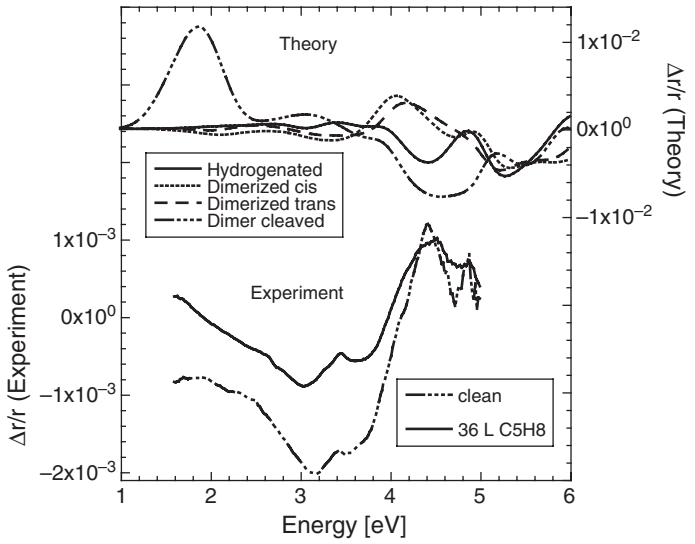

Figure 4. RAS spectra $[\mathrm{Re}\{(r_{[\bar{1}10]} - r_{[110]})/\langle r\rangle\}]$ calculated for Si(001):cyclopentene configurations from [30] are compared with experimental results obtained for the clean and 36 Langmuir cyclopentene-treated Si(001) surface.

cyclopentene-covered Si(001) surface are shown in figure 4. Only the dimer-cleaved structure gives rise to an optical anisotropy in the low-energy region, due to the existence of unsaturated Si surface states. No such states exist in the cases of the dimerized and hydrogenated interface models. Accordingly, in the energy range considered in the calculations, these models give rise to stronger optical anisotropies only for higher energies, in particular around the E_2 critical point energy of Si, related to electronic transitions between surface-modified bulk Si wavefunctions. While positive features close to the E_2 energy are observed for the dimerized models (both *cis* and *trans* configurations), negative anisotropies occur for the hydrogenated and the dimer-cleaved models.

These differences should allow for the discrimination between different adsorption scenarios by means of measuring the reflectance anisotropy of cyclopentene-covered Si(001) surfaces. Therefore we performed experiments in a UHV chamber, with a base pressure of $\leqslant 1.5 \times 10^{-10}$ Torr. The Si(001) substrates were cut 4° off into the [110] direction. In order to produce a defined anisotropic surface, the sample was degassed at 600 °C and cleaned by sequential heating cycles up to 850 °C, while keeping the system pressure below $\leqslant 1.5 \times 10^{-9}$ Torr. Low-energy electron diffraction (LEED) revealed a clear (2×1) pattern when the cleaning procedure was completed, indicative of a surface consisting of mainly one domain. The observed spot splitting is consistent with a periodic double-step structure. Cyclopentene (Fluka, $\geqslant$98.5%) was cleaned by several freeze–pump–thaw cycles and dosed via a leak valve. RAS spectra were taken *in situ* before, during and after dosing with cyclopentene. The experimental RAS set-up is described in detail in [62].

The experimental results, also shown in figure 4, indicate that the step-related negative anisotropy at around 3 eV is weakened upon cyclopentene adsorption on Si(001). The influence of steps on the RAS spectra [12] is not considered in the present calculations for cyclopentene adsorption, hindering the comparison between experiment and theory in the low-energy region. Furthermore, the calculated anisotropies are considerably larger than measured, indicative of defects and superposition of differently reconstructed domains. Nevertheless, the fact

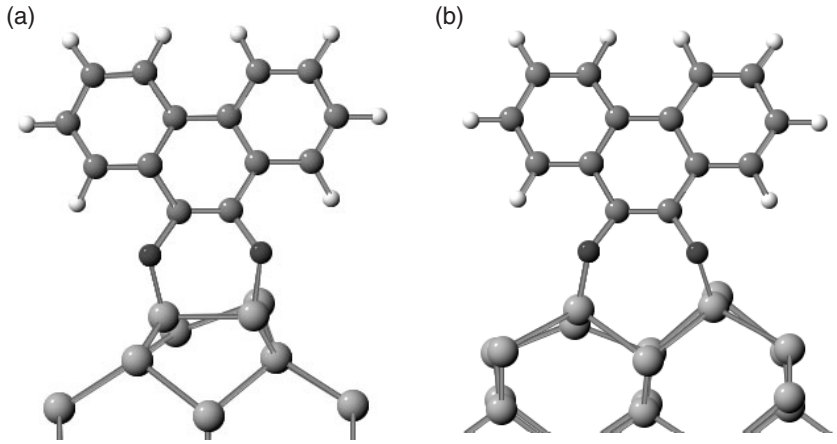

Figure 5. Perspective view of 9,10-phenanthrenequinone adsorbed on Si(001) either in TD (a) or CD geometry (b). White, grey, dark and large grey symbols indicate H, C, O and Si atoms, respectively.

that the positive anisotropy at the E_2 critical point energy seems to be barely affected by cyclopentene adsorption excludes the hydrogenated and dimer-cleaved interface structures as structural candidates. Both show pronounced negative anisotropies in this energy region. The comparison between experiment and theory thus indicates that cyclopentene adsorbs via a [2 + 2] cycloaddition reaction, leaving the Si dimer intact. On the basis of the existing data, however, we cannot discriminate between *cis* and *trans* configurations. Unfortunately, no electronic transitions within the organic layer, i.e., intra- or intermolecular transitions occur within the energy range probed computationally and experimentally.

In order to explore the influence of intramolecular electronic transitions on the RAS signal of organic thin films, we model the adsorption of 9,10-phenanthrenequinone (PQ) on Si(001). This system has been studied experimentally by means of x-ray photoemission spectroscopy, Fourier-transformed infrared spectroscopy, STM [63], ultraviolet photoemission spectroscopy and RAS [56]. Based on these experiments it was suggested that PQ adsorbs via a heteroatomic [4 + 2] Diels–Alder reaction and is attached parallel to the Si surface dimers as shown in figure 5(a). This involves the formation of a six-membered ring containing two silicon, two oxygen and two carbon atoms. As an alternative, we also considered the possibility that the PQ molecule is attached to two Si dimers, in the configuration shown in figure 5(b). Both adsorption configurations, denoted top dimer (TD) and cross dimer (CD) in the following, were studied for coverages of 0.25 and 0.5 monolayers (ML), corresponding to one or two PQ molecules adsorbed in a c(4 × 2) unit cell of Si(001). Higher coverages than these are energetically unfavourable, due to steric repulsion between the molecules.

The calculated and measured changes of the Si(001) RAS signal upon adsorption of PQ molecules are shown in figure 6. Because there are no self-energy corrections included in the RAS calculations, different energy scales have been used for experiment and theory, in order to account approximately for the DFT bandgap problem [38]: self-energy corrections and excitonic effects in the PQ molecule lead to a blueshift of the DFT results by about 0.3 eV, as estimated from ΔSCF (or constrained DFT) calculations for the HOMO–LUMO transition of gas-phase PQ. On the other hand, the calculated values for the Si bulk E_1 and E_2 critical point energies lie about 0.5 eV below the experimental values. We therefore use a rigid offset of 0.4 eV of the upper and lower abscissa in figure 6.

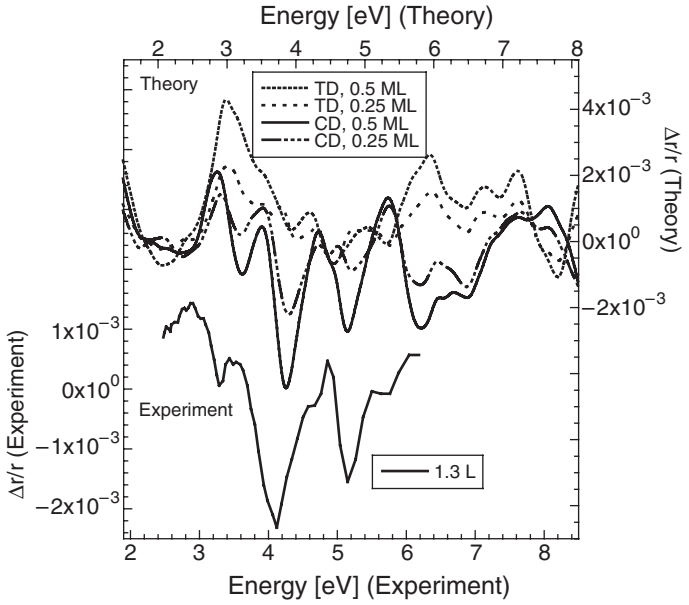

Figure 6. RAS spectra [Re{$(r_{[\bar{1}10]} - r_{[110]})/\langle r\rangle$}] calculated for the Si(001):9,10-phenanthrenequinone configurations shown in figure 5 in comparison with experimental data taken from [56]. Both the experimental and theoretical curves refer to difference spectra, i.e., the RAS of the clean Si(001) sample has been subtracted. The calculated curves haven been rigidly shifted by 0.4 eV to compare with experiment (see text).

As expected, the changes of the RAS signal are roughly proportional to the molecular coverage: they are much stronger for the 0.5 ML adsorption compared to the 0.25 ML case. Pronounced changes occur for photon energies close to the calculated E_1 critical point energy, due to modifications of the Si bulk wavefunctions. Irrespective of the adsorption geometry, PQ adsorption leads to a decrease of the E_1 anisotropy in all investigated cases. In the energy range between E_1 and E_2 (calculated at about 3.0 and 3.8 eV, respectively) we find the RAS signal to be geometry specific. The Si(001) E_2 anisotropy is strongly affected upon PQ adsorption in CD configuration, but barely changes if the adsorption occurs in the TD geometry. Above about 5 eV we find the spectral changes of the TD geometries to nearly mirror the ones induced by adsorption in CD configuration. This indicates that in this energy window the surface optical response is mainly determined by intramolecular transitions. This is confirmed by separate calculations on gas-phase PQ molecules. This energy range is thus particularly well suited to probe the orientation of the molecules with respect to the substrate, whereas the optical response at lower energies contains information about the molecule–substrate bonding. Hacker and Hamers attribute the negative peak at 5.2 eV in the measured RAS spectrum to molecular π–π^* transitions [56]. Self-energy corrections and excitonic effects in the PQ molecule lead to a blueshift of the DFT results of several tenths of an electron-volt, as discussed above. Therefore it appears meaningful to associate the experimental peak at 5.2 eV with the 4.8 eV feature occurring in the DFT-GGA spectrum. The comparison of RAS experiment and theory would then support an adsorption geometry where the PQ molecules adsorb in CD geometry, as shown in figure 5(b). However, a more detailed analysis of the origin of the calculated RAS peaks and the surface thermodynamics and reaction kinetics is needed (and is presently being performed) in order to definitely determine the adsorption geometry.

4. Conclusions

We have performed *first-principles* calculations on the structure and optical properties of oxidized and 9,10-phenanthrenequinone adsorbed Si(001) surfaces as well as measurements of the reflectance anisotropy of Si(001) exposed to cyclopentene. Our results for oxidized Si(001) allow for the qualitative understanding of the experimentally observed RAS oscillation during layer-by-layer oxide growth. They are interpreted in terms of oxygen-induced change of the microscopic surface potential. Our results for organic molecule adsorption show a strong sensitivity of RAS with respect to the geometric details of the bonding. A comparison of measured and calculated spectra for cyclopentene adsorbed on Si(001) indicates a bonding geometry where cyclopentene bonds parallel to the Si surface dimers, with the dimers remaining intact. The comparison between experiment and theory for adsorption of 9,10-phenanthrenequinone points to a structure where the molecules bond to two Si surface dimers.

Acknowledgments

Grants of computer time from the DoD Challenge Program, the Leibniz-Rechenzentrum München and the Höchstleistungsrechenzentrum Stuttgart are gratefully acknowledged. We thank the Deutsche Forschungsgemeinschaft for financial support (SCHM-1361/6), as well as US DoE and ONR.

References

[1] Kamiya I, Aspnes D E, Tanaka H, Florez L T, Harbison J P and Bhat R 1992 *Phys. Rev. Lett.* **68** 627
[2] Kamiya I, Aspnes D E, Florez L T and Harbison J P 1992 *Phys. Rev.* B **46** 15894
[3] Dietz N, Rossow U, Aspnes D E and Bachmann K J 1995 *J. Electron. Mater.* **24** 1571
[4] Zettler J, Haberland K, Zorn M, Pristovsek M, Richter W, Kurpas P and Weyers M 1998 *J. Cryst. Growth* **195** 151
[5] Kress C, Shkrebtii A I and Del Sole R 1997 *Surf. Sci.* **377** 398
[6] McIntyre J D E and Aspnes D E 1971 *Surf. Sci.* **24** 417
[7] Bagchi A, Barrera R G and Rajagopal A K 1979 *Phys. Rev.* B **20** 4824
[8] Del Sole R 1981 *Solid State Commun.* **37** 537
[9] Del Sole R and Fiorino E 1984 *Phys. Rev.* B **29** 4631
[10] Manghi F, Del Sole R, Selloni A and Molinari E 1990 *Phys. Rev.* B **41** 9935
[11] Schmidt W G and Bernholc J 2000 *Phys. Rev.* B **61** 7604
[12] Schmidt W G, Bechstedt F and Bernholc J 2001 *Phys. Rev.* B **63** 045322
[13] Hahn P H, Schmidt W G and Bechstedt F 2002 *Phys. Rev. Lett.* **88** 016402
[14] Schmidt W G, Glutsch S, Hahn P H and Bechstedt F 2003 *Phys. Rev.* B **67** 085307
[15] Palummo M, Pulci O, Marini A, Del Sole R, Hahn P H, Schmidt W G and Bechstedt F 2004 *J. Phys.: Condens. Matter* **16** S4373
[16] Del Sole R and Onida G 1999 *Phys. Rev.* B **60** 5523
[17] Pulci O, Onida G, Del Sole R and Reining L 1998 *Phys. Rev. Lett.* **81** 5374
[18] Schmidt W G, Briggs E L, Bernholc J and Bechstedt F 1999 *Phys. Rev.* B **59** 2234
[19] Schmidt W G, Fattebert J L, Bernholc J and Bechstedt F 1999 *Surf. Rev. Lett.* **6** 1159
[20] Schmidt W G, Bernholc J and Bechstedt F 2000 *Appl. Surf. Sci.* **166** 179
[21] Schmidt W G, Bechstedt F, Fleischer K, Cobet C, Esser N, Richter W, Bernholc J and Onida G 2001 *Phys. Status Solidi* **188** 1401
[22] Schmidt W G, Bechstedt F and Bernholc J 2002 *Appl. Surf. Sci.* **190** 264
[23] Schmidt W G, Esser N, Frisch A M, Vogt P, Bernholc J, Bechstedt F, Zorn M, Hannappel T, Visbeck S, Willig F and Richter W 2000 *Phys. Rev.* B. **61** R16335
[24] Schmidt W G, Bechstedt F, Lu W and Bernholc J 2002 *Phys. Rev.* B **66** 085334
[25] Schmidt W G, Hahn P H, Bechstedt F, Esser N, Vogt P, Wange A and Richter W 2003 *Phys. Rev. Lett.* **90** 126101
[26] Hahn P H, Schmidt W G, Bechstedt F, Pulci O and Del Sole R 2003 *Phys. Rev.* B **68** 033311
[27] Hogan C, Paget D, Tereshchenko O, Reining L and Onida G 2004 *Phys. Rev.* B **69** 125332

[28] Paget D, Hogan C, Berkovits V and Tereshchenko O 2003 *Phys. Rev.* B **67** 245313
[29] Nakayama T and Murayama M 2000 *Appl. Phys. Lett.* **77** 4286
[30] Lu W, Schmidt W G and Bernholc J 2003 *Phys. Rev.* B **68** 115327
[31] Silvestrelli P, Pulci O, Palummo M, Del Sole R and Ancilotto F 2003 *Phys. Rev.* B **68** 235306
[32] Seino K and Schmidt W G 2004 *Surf. Sci.* **548** 183
[33] Kresse G and Furthmüller J 1996 *Comput. Mater. Sci.* **6** 15
[34] Perdew J P, Chevary J A, Vosko S H, Jackson K A, Pederson M R, Singh D J and Fiolhais C 1992 *Phys. Rev.* B **46** 6671
[35] Preuss M, Schmidt W G, Seino K, Furthmüller J and Bechstedt F 2004 *J. Comp. Chem.* **25** 112
[36] Seino K, Schmidt W G, Furthmüller J and Bechstedt F 2002 *Phys. Rev.* B **66** 235323
[37] Adolph B, Furthmüller J and Bechstedt F 2001 *Phys. Rev.* B **63** 125108
[38] Bechstedt F 1992 *Festköperprobleme/Advances in Solid State Physics* vol 32, ed U Rössler (Braunschweig/Wiesbaden: Vieweg) p 161
[39] Schmidt W G, Bechstedt F and Bernholc J 2000 *J. Vac. Sci. Technol.* B **18** 2215
[40] Briggs E L, Sullivan D J and Bernholc J 1996 *Phys. Rev.* B **54** 14362
[41] Bernholc J, Briggs E L, Bungaro C, Nardelli M B, Fattebert J L, Rapcewicz K, Roland C, Schmidt W G and Zhao Q 2000 *Phys. Status Solidi* b **217** 685
[42] Hamann D R 1989 *Phys. Rev.* B **40** 2980
[43] Yasuda T, Yamasaki S, Nishizawa M, Miyata N, Shklyaev A, Ichikawa M, Matsudo T and Ohta T 2001 *Phys. Rev. Lett.* **87** 037403
[44] Yasuda T and Kagaku H 2002 *J. Surf. Sci. Soc. Japan* **23** 562
[45] Mantese L, Bell K A, Rossow U and Aspnes D E 1998 *Thin Solid Films* **313/314** 557
[46] Hingerl K, Balderas-Navarro R E, Hilber W, Bonanni A and Stifter D 2000 *Phys. Rev.* B **62** 13048
[47] Hingerl K, Balderas-Navarro R E, Bonanni A, Tichopadek P and Schmidt W G 2001 *Appl. Surf. Sci.* **175/176** 769
[48] Yamasaki T, Kato K and Uda T 2003 *Phys. Rev. Lett.* **91** 146102
[49] Shioda R and van der Weide J 1998 *Phys. Rev.* B **57** R6823
[50] Kipp L, Biegelsen D K, Northrup J E, Swartz L-E and Bringans R D 1996 *Phys. Rev. Lett.* **76** 2810
[51] Yasuda T, Mantese L, Rossow U and Aspnes D E 1995 *Phys. Rev. Lett.* **74** 3431
[52] Jaloviar S G, Lin J-L, Liu F, Zielasek V, McCaughan L and Lagally M G 1999 *Phys. Rev. Lett.* **82** 791
[53] Wolkow R A 1999 *Annu. Rev. Phys. Chem.* **50** 413
[54] Sassella A, Borghesi A, Meinardi F, Tubono R, Gurioli M, Botta C, Porzio W and Barbarella G 2000 *Phys. Rev.* B **62** 11170
[55] Paraian A M, Rossow U, Park S, Salvan G, Friedrich M, Kampen T U and Zahn D R T 2001 *J. Vac. Sci. Technol.* B **19** 1658
[56] Hacker C A and Hamers R J 2003 *J. Phys. Chem.* B **107** 7689
[57] Hamers R J, Hovis J S, Lee S, Liu H and Shan J 1997 *J. Phys. Chem.* B **101** 1489
[58] Hovis J S, Lee S, Liu H and Hamers R J 1997 *J. Vac. Sci. Technol.* B **15** 1153
[59] Lee S W, Hovis J S, Coulter S K, Hamers R J and Greenlief C M 2000 *Surf. Sci.* **462** 6
[60] Akagi K and Tsuneyuki S 2001 *Surf. Sci.* **493** 131
[61] Cho J-H and Kleinman L 2001 *Phys. Rev.* B **64** 235420
[62] Rossow U and Richter W 1996 *Optical Characterisation of Epitaxial Semiconductor Layers* ed G Bauer and W Richter (Berlin: Springer) pp 43–52
[63] Fang L, Liu J, Coulter S, Cao X, Schwartz M P, Hacker C and Hamers R J 2002 *Surf. Sci.* **514** 362